

# Structure and Growth of Ultrasmall Protein Microcrystals by Synchrotron Radiation: II. $\mu$ GISAX and Microscopy of Lysozyme

Eugenia Pechkova<sup>1,2</sup> and Claudio Nicolini<sup>1,2\*</sup>

<sup>1</sup>Fondazione EL.B.A., via delle Testuggini snc, 00187 Roma, Italy

<sup>2</sup>Nanoworld Institute and Biophysics Division, University of Genoa, Corso Europa 30, 16132 Genoa, Italy

**Abstract** The early steps of growth and nucleation of the lysozyme microcrystals by classical and nanotemplate-based hanging vapor diffusion methods are studied using  $\mu$ GISAXS at the European Synchrotron Radiation Facility (ESRF) in Grenoble, France. Out-of-plane cuts in the Yoneda regions of the 2D scattering profiles point to the detection of ultrasmall lysozyme crystals by  $\mu$ GISAXS quite before than by light microscopy. Furthermore lysozyme crystal formation occurs quite earlier with the nanotemplate than with the classical method. Our data are compatible with two distinct modes of crystal nucleation and growth for P450sc and lysozyme. *J. Cell. Biochem.* 97: 553–560, 2006.

© 2005 Wiley-Liss, Inc.

**Key words:** synchrotron radiation; microbeam grazing incidence scattering; lysozyme microcrystals; microscopy

Many proteins playing a key role in living mechanisms have not yet been crystallized, and the growth of these crystals is the rate-limiting factor for their structural determination. New rational methodologies and protocols to produce and characterize single, high-quality protein crystals are thereby needed. Recently the production of stable radiation resistant protein microcrystals by nanobiofilm template has opened new avenues [Pechkova and Nicolini, 2003, 2004; Pechkova et al., 2004]. This is made possible by the introduction of instrumentation and microfocus beamline for X-ray crystal analysis capable to study very small crystals of only a few microns in size using third generation synchrotrons [Müller-Buschbaum et al., 2003].

The combination of the above two new technologies is discussed in a recent opinion article [Pechkova and Nicolini, 2004] and book [Pechkova and Nicolini, 2003], providing a route to determine the structures of proteins and protein complexes that have not yet been characterized. Here we investigate the utilization of a new microbeam grazing incidence small-angle X-ray scattering [Roth et al., 2003] for understanding the basic physical aspects of the template induced microcrystal nucleation and growth, as compared to the classical vapor diffusion method [Ducruix and Giege, 1999].  $\mu$ GISAXS is indeed an excellently suited method to study the initial stages of crystal growth and nucleation at the interface between the film substrate and the protein solution in the droplet on the nm-scale [Roth et al., 2003]. As scanning force microscopy (SFM), sensitive only to surface structures [Pechkova and Nicolini, 2003], grazing incidence small-angle X-ray scattering ( $\mu$ GISAXS) appears optimal for structural and morphological studies of patterned thin films [Müller-Buschbaum et al., 1998, 2000]. Atomic force microscopy (AFM) has been frequently used to study protein and viruses crystals in situ, in their mother liquors, as they grown. By means of these AFM studies, biological macromolecules appear to utilize a more diverse range of growth mechanisms in

Grant sponsor: FIRB-MIUR grant on Organic Nanoscience and Nanotechnology to the Nanoworld Institute; Grant sponsor: The Fondazione EL.B.A.; Grant sponsor: The Centro Interuniversitario di Ricerca sulle Nanotecnologie e Nanoscienze Organiche e Biologiche of Genova University.

\*Correspondence to: Claudio Nicolini, Nanoworld Institute and Biophysics Division, University of Genoa, Corso Europa 30, 16132 Genoa, Italy.

E-mail: manuscript@ibf.unige.it

Received 10 January 2005; Accepted 28 April 2005

DOI 10.1002/jcb.20538

© 2005 Wiley-Liss, Inc.

their crystallization than any previously studied materials. More recently from the sequential AFM images taken at brief intervals over many hours, or even days, the mechanisms and kinetics of the growth process have been recently defined [McPherson et al., 2003]. The appearance of both two- and three-dimensional nuclei on crystal surfaces have been visualized, defect structures of crystals were clearly evident, and defect densities of crystals were also determined.

Another technique was also developed employing the AFM in the linescan mode to observe growth events on protein crystal faces in real time. This technique can be used to measure the growth unit sizes on protein crystal faces as well, allowing their molecular growth mechanisms to be determined experimentally. It was applied to probe the growth mechanism of the (110) face of tetragonal lysozyme crystals [Li et al., 1999]; in this study the latest step of crystal growth is observed, often on the large crystal terrace [Yip et al., 2000].

Further research is however needed to investigate the early steps of protein crystallization and for this reason we concentrate on the  $\mu$ GISAXS method which appear potentially able to utilize the out-of-plane cuts in the Yoneda regions of its 2D scattering profiles in order to detect ultrasmall lysozyme crystals quite before the light microscopy.  $\mu$ GISAXS is indeed not restricted to the sample's surface, but is sensitive to structures within the penetration depth of X-rays impinging at small angles (grazing incidence) on a sample surface [Müller-Buschbaum et al., 1998, 2000]. In particular, its potential in

nondestructively determining the structure and morphology of patterned thin protein films is exploited due to its order of-magnitude increase in the achievable resolution compared to conventional SAXS experiments [Roth et al., 2003].

## MATERIALS AND METHODS

### Homologous Nanobiofilm Template

The set up conditions for lysozyme crystallization have been previously given in Pechkova and Nicolini [2001]. As shown in the accompanying paper [Nicolini and Pechkova, 2005] the protein thin-film nanotemplate is created using Langmuir-Blodgett (LB) technology or modifications of it (Nicolini, 1997) and is deposited on a solid glass support, to be subsequently placed in the appropriate vapour-diffusion apparatus as a modification of the "classical" hanging drop vapour-diffusion method [Ducruix and Giege, 1999]. This thin LB protein film acts as nanostructured template for protein crystal nucleation and growth up to 1,000 micron size. This heterogeneous crystallization reduces the level of supersaturation, allowing acceleration of lysozyme crystal nucleation and growth [Pechkova and Nicolini, 2001]. Moreover, this method seems to produce radiation stable crystals [Pechkova et al., 2004], quite more resistant than those obtained by classical techniques. This aspect concerns also the crystals of miniscule thickness dimensions (10–20 micron), such as those used for human kinase 3D structure determination by synchrotron microfocus diffraction [Pechkova et al., 2003]. In the present

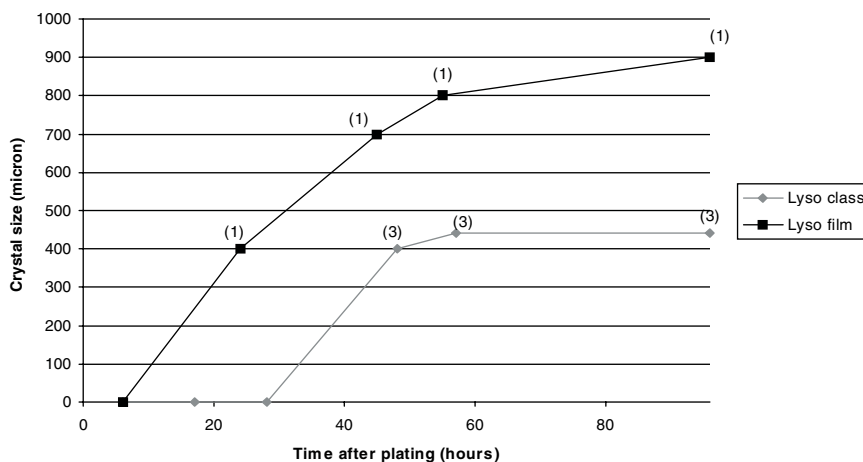


**Fig. 1.** The best case for lysozyme crystal size measured by light microscopy (in microns) versus time (in hours) after plating utilizing the classical and the nanotemplate-based vapor diffusion method.

work, the data are obtained also with the standard vapor diffusion hanging method called "classical" [Ducruix and Giege, 1999]. Every 10  $\mu$ l drop contains equal proportion of lysozyme containing solution of  $\text{CH}_3\text{COONa}$  pH 4.5 and of  $\text{CH}_3\text{COONa}$  0.9 M NaCl pH 4.5.

### Microbeam Grazing Incidence X-Ray Scattering

The experimental procedure and the schematic picture of the  $\mu$ GISAXS setup are shown in Figure 1 of the accompanying paper [Nicolini and Pechkova, 2005], where the sample is mounted on a xyz-gantry and a two-axis goniometer. The incoming monochromatic X-ray beam ( $\lambda = 0.9775 \text{ \AA}$ ) is 5  $\mu$  wide, and a two-dimensional (2-D) high-resolution detector records the scattered intensity from the sample surface. In the 2-D pattern, structural variations in  $z$  (depth of the sample), for example, a finite surface roughness, lead to a specular and off-specular scattered intensity in  $q_z$ -direction. Structures in the  $x$ - $y$  plane lead to out-of-plane (with respect to the incoming beam and the

sample surface normal) signals with finite  $q_y$  and  $2\theta \neq 0$ . Thin films investigated by GISAXS so far [Holy and Baumbach, 1994] were of limited spatial resolution due to the large beam size available (several hundred micrometers) [Gehrke, 1992]. As shown earlier [Roth et al., 2003] and in the accompanying paper [Nicolini and Pechkova, 2005], to investigate our protein drops we utilized  $\mu$ GISAXS combining a micrometer-sized synchrotron beam with a specifically designed low-background GISAXS setup [Sennett and Scott, 1950; Riekel, 2000; Lazzari, 2002]. Typically the data were acquired at  $0.88^\circ$  incident angle in a time ranging between 7 and 20 min to avoid amorphous protein precipitation and salt crystals.

### RESULTS

We systematically investigate the kinetics of the nanometer-sized crystals being formed with and without nanobiofilm template of homologous proteins. We used Lysozyme as it can be

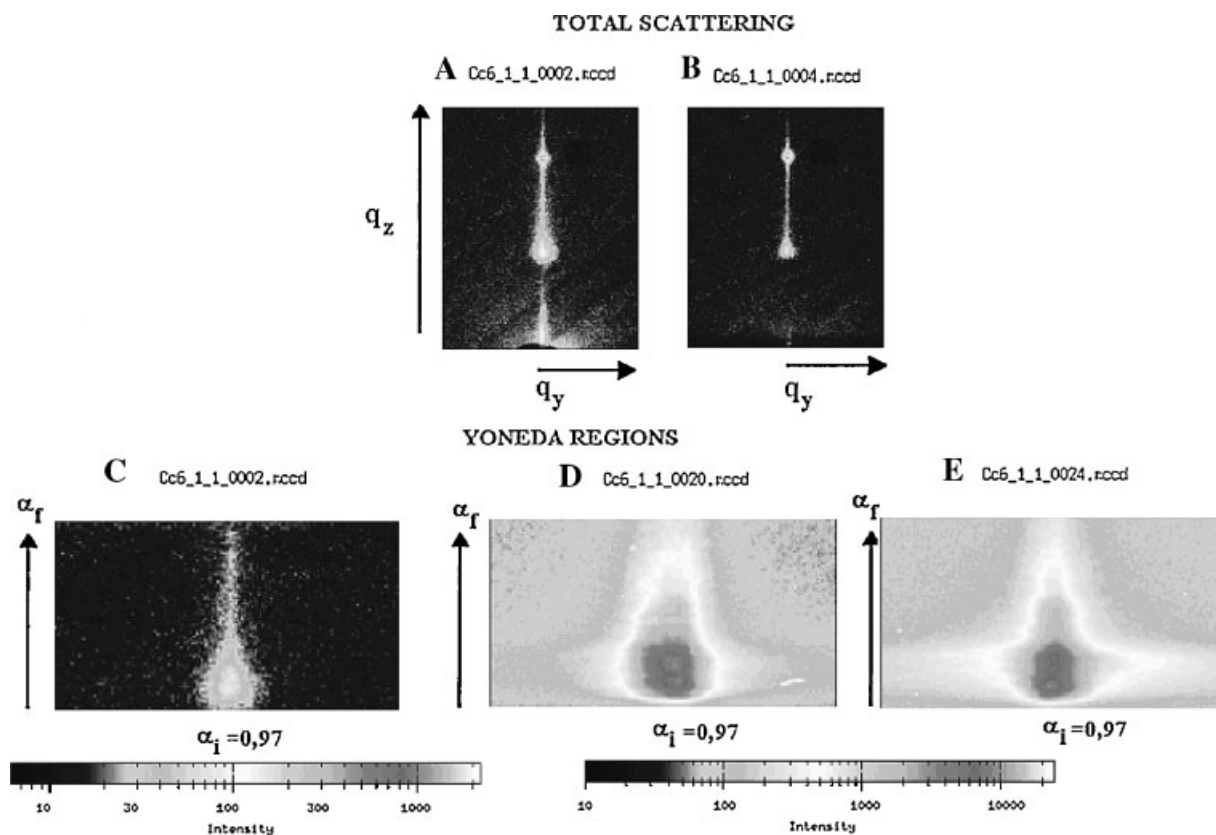


**Fig. 2.**  $\mu$ GISAXS images of lysozyme drop at 30 h after plating with nanotemplate-assisted hanging vapor diffusion method, taken at successive time intervals to monitor the evaporation of protein drop solution and the corresponding formation of layers of protein crystals and then of salt crystals. **A:** total  $\mu$ GISAXS patterns. **B:** the Yoneda regions.

easily crystallized and can thus be used as model system to monitor the time-dependent crystals growth in size and number as evaluated by light microscopy (Fig. 1), in correlation with  $\mu$ GISAXS measurements (Figs. 2–4). During a series of parallel experiments, the lysozyme crystals appear to grow in size with time, and significantly better for the nanotemplate-assisted method, but not in number, which appears to remain constant (Fig. 1).

Under the same conditions of buffer solution and temperature, the  $\mu$ GISAXS images of the 10  $\mu$ l lysozyme drop appear to change significantly along the y-axis whenever successively

acquired at equally spaced time intervals over 7 min, likely due to sedimentation processes of both protein crystals and salt solution (Fig. 2).

For this reason, in order to compare the crystallization process taking place with time in presence and absence of protein nanotemplate, we kept constant the measuring time, carrying out the measurements quite rapidly immediately after removal from the container where the lysozyme crystals are formed (see Fig. 1 of Nicolini and Pechkova, 2005). A drop containing only buffer solution with salt and precipitant lacks any peak and appears quite less intense with diffuse low scattering signal

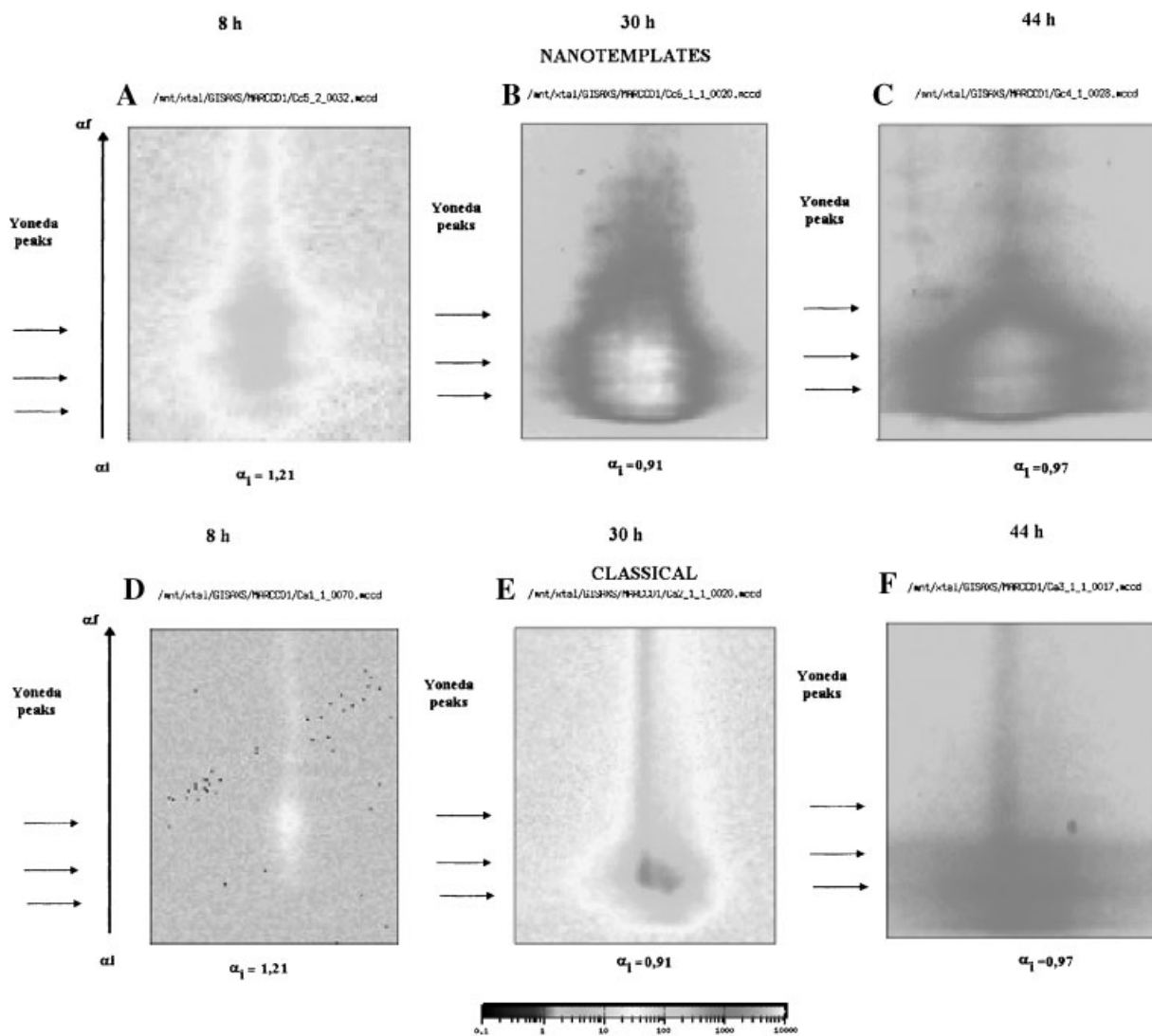


**Fig. 3.** Yoneda regions of Lysozyme “nanotemplate based” (A, B, C) versus “classical” (D, E, F) drops taken at 8, 30, and 43 h after plating are indicated with arrows. The patterns of  $\alpha_1$  dependency at different  $\alpha_1$  are shown on a logarithmic scale to enhance the features in the Yoneda regions.

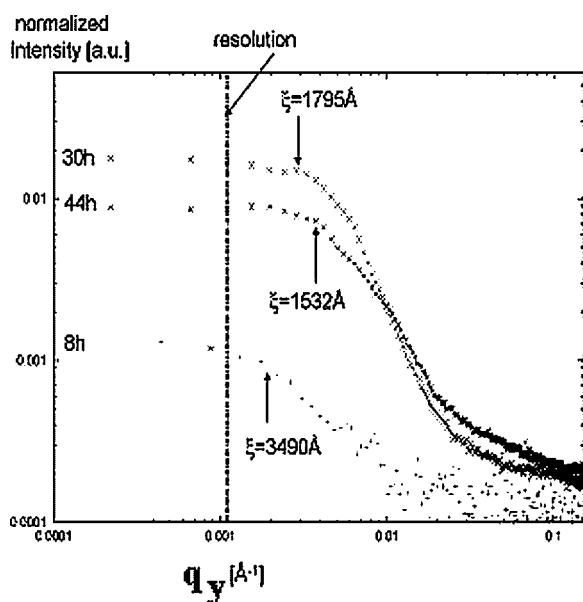


**Fig. 4.** Out-of-plane scans of the Yoneda regions of the nanotemplate-assisted samples at 8, 30, and 44 h after plating. Included are the template and the glass substrate. Clearly the enhancement of the diffuse scattering with increasing time is visible. The detector dark noise has been subtracted and the intensity normalized to the acquisition time. Curve 8h is shifted for clarity. The arrows indicate most-prominent in-plane lengths  $\xi$ . The resolution is marked by a vertical line.

(not shown). The same effect is apparent in the Yoneda regions which represent a characteristic feature of  $\mu$ GISAXS [Yoneda, 1963].

We investigated three crystallization times after plating at 7, 30, and 43 h, which are visualized on a logarithmic time scale in Figure 3, for both the nanotemplate-assisted and the classical hanging drop vapor diffusion methods. To minimize time loss due to adjustment, the samples were rapidly adjusted to an incident angle around  $1^\circ$  being large enough to make clear the important features. In the nanotemplate-assisted samples a significant progressive enlargement of the corresponding  $\mu$ GISAXS pattern with time after plating appears for both the overall raw data acquired (Fig. 2A–B) and the enhanced Yoneda region (Figs. 2C–E and 3A–E), which appears not only quite larger at increasing time interval but also significantly present of the highest  $\alpha_f$  peak even at 7 h after plating when no crystal can be observed at the light microscope. Thereby we cannot rule out the possibility that the higher angle Yoneda peak stems from the glass substrate.

Only at the lowest  $\alpha_f$  peaks similar building up effect is apparent in both the “nanotemplate”

and “classical” samples, where in the latter at 30 h a significant  $\mu$ GISAXS signal is moreover present even when the light microscope fails to observe any lysozyme crystal. It must be noticed that no thin protein film is present in the classical sample but only the glass where the drop is sitted: interestingly no signal is apparent in the intermediate second Yoneda peak of the classical sample.

The Yoneda region (Fig. 3) appears most sensitive to structural and morphological changes of the surfaces due to the interference effect involved in the occurrence of the Yoneda [Yoneda, 1963], with the  $\mu$ GISAXS pattern being scaled to the same scatter intensity. At 7 h, clearly two other Yoneda peaks emerges with lower critical angle in the nanotemplate-assisted samples but not in the classical one. From the comparison of Figure 3a with Figure 3d one can thereby exclude that the lower peaks are due to the salt (NaAc) precipitating on the glass substrate thus forming a new rough layer of small crystals. This could lead us to attribute the peak at intermediate  $\alpha_f$  values, not apparent in the classical sample, to that of the protein film substrate with roughness increased by holes over the time. The lowest  $\alpha_f$ -values could correspond to protein crystal being formed by the removal of proteins from the nanotemplate. Even if this interpretation is compatible with the  $\mu$ GISAXS experiments on P450sc [Nicolini and Pechkova, 2005], we do not have them with enough statistics to give an absolute certainty to this interpretation.

The newly developing peak with the lowest  $\alpha_f$  values thus seems to be related with the crystal protein itself.

Furthermore, we performed out-of-plane cuts at the position of the Yoneda peak. The results are depicted in Figure 4. The out-of-plane cuts can indicate a most-prominent in-plane length scale  $\xi$ . In our case there seems to be a shoulder around  $q$ -values larger than the resolution, which is set conservatively to  $q_{\min} = 0.0012 \text{ \AA}^{-1}$  corresponding to a maximum resolvable real space length of  $\xi_{\max} = 5712 \text{ \AA}$ . In our case one could calculate for 8, 30, 44 h most-prominent in-plane lengths of  $\xi_8 = 3490 \text{ \AA}$ ,  $\xi_{30} = 1795 \text{ \AA}$ ,  $\xi_{44} = 1532 \text{ \AA}$ . Clearly  $\xi$  is decreasing with plating time.

The object of this manuscript is also the comparison of the results derived from these ex-situ lysozyme  $\mu$ GISAXS studies with the

ex-situ cytochrome P450scc microcrystals shown in the accompanying paper [Nicolini and Pechkova, 2005] in order to draw conclusions on the early steps and the differential mechanisms for nucleation and growth of these two different protein systems.

By monitoring also the differential size and number of microcrystal dependence as function of time for both P450scc (Fig. 5) and Lysozyme (Figs. 1 and 5), two models could then be proposed for the mechanism of crystal growth and nucleation, both yielding a similar decrease in the in-plane length scale  $\xi$  with time after plating, displaying one an increase in crystal

size with constant crystal number, and the other an increase in the number of crystals with approximately constant size (Fig. 6). As shown by Figure 1 lysozyme crystal growth and nucleation, at least in this series of experiments being carried out in parallel with  $\mu$ GISAXS measurements, is compatible with the first while the cytochrome crystal growth and nucleation (Fig. 5) is compatible with the latter.

## CONCLUSIONS

The  $\mu$ GISAXS allows for a nondestructive and contact-free reconstruction of the structure and

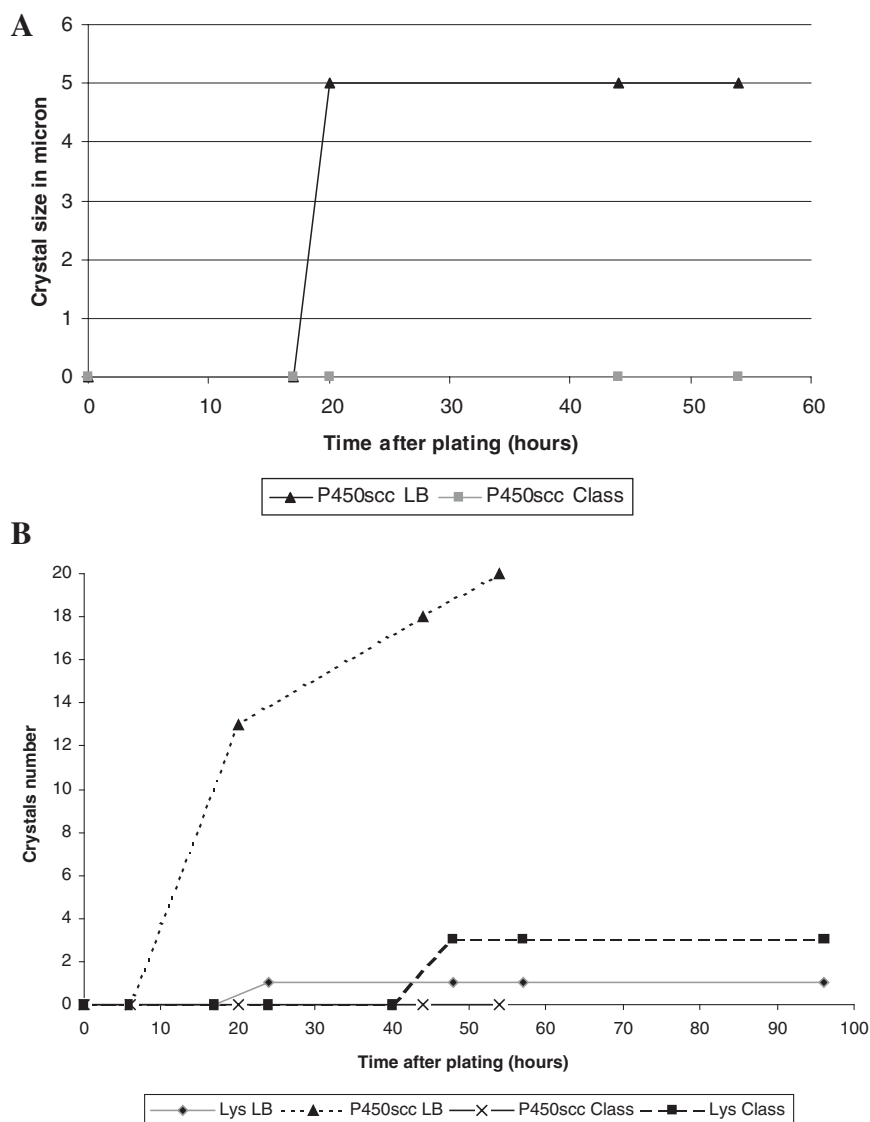


**Fig. 5.** The typical case for crystal size (in microns) and number versus time (in hours) after plating of the same  $\mu$ GISAX samples of P450scc (A) and Lysozyme (B) in classical versus nanotemplate-based vapor diffusion method.

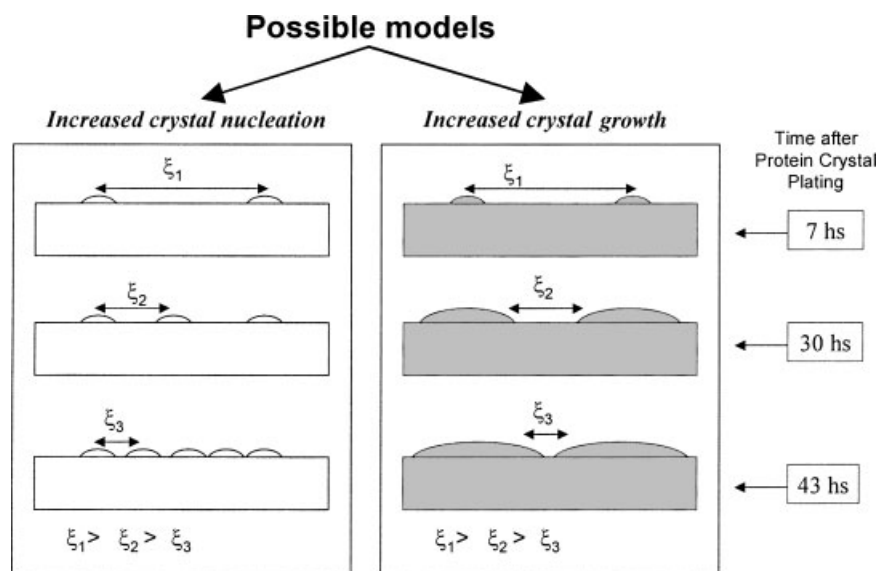


Fig. 6. Alternative models of crystal nucleation and growth.

morphology of extra small crystals, quite smaller than those observable by light microscopy (Figs. 1 and 5). It monitors also the alterations occurring within the thin film acting as substrate (Figs. 2–4) and as template for their induced growth acceleration (Fig. 1). In Figure 2, the time scan shows a strong lateral diffuse scattering which changes in time after the first 20 successive images were acquired at 30 s interval, suggesting that the material sediments only after the first 10 min in the 10  $\mu$ l drop. This shows, thereby, that  $\mu$ GISAXS scans have a meaning in ex-situ experiments by measuring the very first images, considering that no or only little material sediments in the first 10 min! Hence, Figure 4 has physical meaning and might be related to the crystal nucleation and growth and not only the occurrence of the Yoneda peaks at  $q_y = 0$ . This suggests that in-situ experiments being planned are useful but not indispensable, in order to produce data not disturbed by sedimentation!

Due to the unique combination of GISAXS and micrometer sized beam, our investigation of lysozymes confirms the higher performance of the nanotemplate method in producing crystals and provides new insights on the differential early steps of crystal nucleation and growth within the drop for both the lysosymes and the cytochromes.  $\mu$ GISAXS data allow indeed monitoring crystal formation at a resolution and a scale previously unmatched even with respect to what has been significantly achieved by AFM

studies [Li et al., 1999; Yip et al., 2000; McPherson et al., 2003].

#### ACKNOWLEDGMENTS

We are grateful for the cooperation of Christian Riekkel, Manfred Burghammer and Stephan Roth of ESRF in acquiring the  $\mu$ GISAXS data at the ID13 of the ESRF in Grenoble.

#### REFERENCES

- Ducruix A, Giege R. 1999. Crystallization of nucleic acids and proteins. A practical approach. New York: Oxford University Press. pp 130–133.
- Gehrke R. 1992. An ultrasmall angle scattering instrument for the DORIS-III bypass. *Rev Sci Instrum* 63:455–458.
- Holy V, Baumbach T. 1994. Nonspecular X-ray reflection from rough multilayers. *Phys Rev B* 49:10668–10676.
- Lazzari R. 2002. IsGISAXS: A program for grazing-incidence small-angle X-ray scattering analysis of supported islands. *J Appl Crystallogr* 35:406–421.
- Li H, Nadarajah A, Pusey ML. 1999. Determining the molecular-growth mechanisms of protein crystal faces by atomic force microscopy. *Acta Crystallographica D* 55: 1036–1045.
- McPherson A, Kuznetsov YuG, Malkin AJ, Plomp M. 2003. Macromolecular crystal growth as revealed by atomic force microscopy. *J Struct Biol* 142:32–46.
- Müller-Buschbaum P, Casagrande M, Gutmann J, Kuhlmann T, Stamm M, von Krosigk G, Lode U, Cunis S, Gehrke R. 1998. Determination of micrometer length scales with an X-ray reflection ultra small-angle scattering set-up. *Europhys Lett* 42:517–519.
- Müller-Buschbaum P, Gutmann JS, Stamm M, Cubitt R, Cunis S, Von Krosigk G, Gehrke R, Petry W. 2000. Dewetting of thin polymer-blend films examined with GISAXS. *Physica B* 283:53–59.

- Müller-Buschbaum P, Roth SV, Burghammer M, Diethert A, Panagiotou P, Riekel C. 2003. Multiple-scaled polymer surfaces investigated with micro-focus grazing incidence small-angle X-ray scattering. *Europhys Lett* 61:639–645.
- Nicolini C. 1997. Protein monolayer engineering: principles and application to biocatalysis. *Trends in Biotechnology* 15:395–401.
- Nicolini C, Pechkova E. 2005. Structure and growth of ultrasmall protein microcrystals by synchrotron radiation: I.  $\mu$ GISAXS and  $\mu$ Diffraction of P450<sub>sec</sub>. *J Cell Biochem* (in press).
- Pechkova E, Nicolini C. 2001. Accelerated protein crystal growth onto the protein thin film. *J Cryst Growth* 231:599–602.
- Pechkova E, Nicolini C. 2003. Proteomics and nanocrystallography. New York: Kluwer-Plenum. pp 1–210.
- Pechkova E, Zanotti G, Nicolini C. 2003. Three-dimensional atomic structure of a catalytic subunit mutant of human protein kinase CK2. *Acta Crystallographica D* 59:2133–2139.
- Pechkova E, Tropiano G, Riekel C, Nicolini C. 2004. Radiation stability of protein crystals grown by nanostructured templates: Synchrotron microfocus analysis. *Spectrochimica Acta B* 59:1687–1693.
- Pechkova E, Roth SV, Fontani D, Riekel C, Nicolini C. 2005.  $\mu$ GISAXS and protein nanotemplate crystallization: Methods and Instrumentation. *J Synchrotron Radiation* (November 2005).
- Riekel C. 2000. New avenues in X-ray microbeam experiments. *Rep Prog Phys* 63:233–262.
- Roth V, Burghammer M, Riekel C, Müller-Buschbaum P, Diethert A, Panagiotou P, Walter H. 2003. Self-assembled gradient nanoparticle-polymer multilayers investigated by an advanced characterization method: Microbeam grazing incidence X-ray scattering. *Appl Phys Lett* 82:1935–1937.
- Sennett RS, Scott GD. 1950. The structure of evaporated metal films and their optical properties. *J Opt Soc Am* 40:203–211.
- Yip CM, Brader ML, Frank BH, De Felippis MR, Ward MD. 2000. Structural studies of a crystalline insulin analog complex with protamine by atomic force microscopy. *Biophys J* 78:466–473.
- Yoneda Y. 1963. Anomalous surface reflection of X-rays. *Phys Rev* 161:2010–2013.